



Spatio-temporal patterns of C : N : P ratios in the northern Benguela upwelling system

A. Flohr¹, A. K. van der Plas², K.-C. Emeis^{3,4}, V. Mohrholz⁵, and T. Rixen⁴

¹Leibniz Centre for Tropical Marine Ecology (ZMT), Fahrenheitstraße 6, 28359 Bremen, Germany

²National Marine Information and Research Centre, Ministry of Fisheries & Marine Resources, P.O. Box 912 Swakopmund, Namibia

³Helmholtz Centre for Materials and Coastal Research Geesthacht, Max-Planck-Straße 1, 21502 Geesthacht, Germany

⁴Institute for Biogeochemistry and Marine Chemistry, University of Hamburg, Bundesstraße 55, 20146 Hamburg, Germany

⁵Leibniz Institute for Baltic Sea Research, Seestraße 15, 18119 Rostock, Germany

Correspondence to: A. Flohr (anita.flohr@zmt-bremen.de)

Received: 3 June 2013 – Published in Biogeosciences Discuss.: 27 June 2013

Revised: 6 December 2013 – Accepted: 18 December 2013 – Published: 14 February 2014

Abstract. On a global scale the ratio of fixed nitrogen (N) and phosphate (P) is characterized by a deficit of N with regard to the classical Redfield ratio of N : P = 16 : 1 reflecting the impact of N loss occurring in the oceanic oxygen minimum zones. The northern Benguela upwelling system (NBUS) is known for losses of N and the accumulation of P in sub- and anoxic bottom waters and sediments of the Namibian shelf resulting in low N : P ratios in the water column. To study the impact of the N : P anomalies on the regional carbon cycle and their consequences for the export of nutrients from the NBUS into the oligotrophic subtropical gyre of the South Atlantic, we measured dissolved inorganic carbon (C_T), total alkalinity (A_T), oxygen (O_2) and nutrient concentrations in February 2011. The results indicate increased P concentrations over the Namibian shelf due to P efflux from sediments resulting in a C : N : P : $-O_2$ ratio of 106 : 16 : 1.6 : 138. N reduction further increase C : N and reduce N : P ratios in those regions where O_2 concentrations in bottom waters are $< 20 \mu\text{mol kg}^{-1}$. However, off the shelf along the continental margin, the mean C : N : P : $-O_2$ ratio is again close to the Redfield stoichiometry. Additional nutrient data measured during two cruises in 2008 and 2009 imply that the amount of excess P, which is created in the bottom waters on the shelf, and its export into the subtropical gyre after upwelling varies through time. The results further reveal an inter-annual variability of excess N within the South Atlantic Central Water (SACW) that flows from the north into the NBUS, with highest N values observed in 2008. It is pos-

tulated that the N excess in SACW occurred due to the impact of remineralized organic matter produced by N_2 fixation and that the magnitude of excess P formation and its export is governed by inputs of excess N along with SACW flowing into the NBUS. Factors controlling N_2 fixation north of the BUS need to be addressed in future studies to better understand the role of the NBUS as a P source and N sink in the coupled C : N : P cycles.

1 Introduction

The biological carbon pump is the term used for the production of organic carbon from dissolved carbon dioxide (CO_2) in the surface mixed layer of the ocean and its transport into the large CO_2 reservoir of the ocean beneath the mixed layer. It is both driven and limited by the availability of macronutrients, such as fixed nitrogen (N) and phosphate (P), as well as micronutrients such as iron (Watson et al., 2000; Behrenfeld et al., 2006b). Macronutrients are required in specific stoichiometric ratios for the photosynthetic production of organic matter, traditionally termed the Redfield ratio of C : N : P = 106 : 16 : 1 (Redfield et al., 1963). Nevertheless, on a more regional scale, phytoplankton C : N : P ratios vary with growth rate, taxonomy, ambient CO_2 concentrations and nutrient availability (e.g. Arrigo, 2005; Riebesell et al., 2007). Especially upon exhaustion of the nutrients, changes in the nutrient uptake ratios could strongly influence

the marine productivity and the oceans ability to sequester CO₂ from the atmosphere (McElroy, 1983; Heinze et al., 1991; Falkowski, 1997).

The ratios of remineralized C, N, P and consumed oxygen (-O₂) (C : N : P : -O₂) are useful to characterize the coupled nutrient and carbon cycling in the oceans. On a global scale the mineralization of nutrients is essentially constant with depth and in good agreement with the traditional Redfield ratio for the photosynthetic production of organic matter (Redfield et al., 1963; Takahashi et al., 1985; Anderson and Sarmiento, 1994). However, depending also on the methods used, variations of the C : N : P : -O₂ mineralization ratios, e.g. with depth have been suggested indicating elemental fractionation during the mineralization of sinking organic matter (Takahashi et al., 1985; Li and Peng, 2002; Schneider et al., 2003; Brea et al., 2004) and an impact of N loss occurring in oxygen minimum zones (OMZ) (Gruber and Sarmiento, 1997; Tyrrell and Law, 1997).

Eastern boundary upwelling systems (EBUS) are regions of high CO₂ concentrations (Boehme et al., 1998; Torres et al., 1999) and intense biological production and export of carbon (Carr, 2002). They also play an important role in supplying nutrients to the surface mixed layer of adjacent oligotrophic subtropical gyres, where nutrient supply is limited by stable thermal stratification (Behrenfeld et al., 2006a). The Benguela upwelling system (BUS) is a coastal upwelling system known for non-standard nutrient (N : P) ratios in upwelling waters (Dittmar and Birkicht, 2001; Tyrrell and Lucas, 2002) caused by N loss (anammox and/or denitrification) and P release from sediments in low-O₂ environments (Kuypers et al., 2005; Nagel et al., 2013). The C : N : P remineralization ratios in the subsurface waters are poorly constrained but are crucial in order to characterize the cycling of C in the BUS.

We analysed nutrient (NO₃⁻, NO₂⁻, P) and dissolved O₂ data in conjunction with data on dissolved inorganic carbon (C_T) and total alkalinity (A_T) produced during an expedition in 2011, and complemented these with nutrient data from two other expeditions staged in 2008 and 2009. Our objectives were to investigate C : N : P : -O₂ mineralization ratios of the northern Benguela upwelling system (NBUS) to study the spatial and temporal impact of N reduction and the associated consequences for the export of nutrients from the eutrophic upwelling system into the oligotrophic subtropical gyre.

2 Material and methods

2.1 Study area

The BUS spans along the southwestern coast of Africa, covering the western South African and Namibian coastline roughly from Cape Agulhas (~ 34° S) to the Angola Benguela Frontal Zone (ABFZ) (Hutchings et al., 2009) (Fig. 1a). At the ABFZ, which is centred between 14 and

16° S (Meeuwis and Lutjeharms, 1990) but is highly dynamic in terms of shape and location, the cold Benguela current system converges with warm tropical waters of the Angola Current (AC). To the south, the system is bordered by the Agulhas Current, which reverses and partly converges with the South Atlantic water, resulting in the formation of eddies (Agulhas rings, AR) and filaments (Hall and Lutjeharms, 2011).

Along the coast of southwestern Africa, the interaction of southerly trade winds with coastal topography forces upwelling, which is strongest at three distinct upwelling cells (Shillington et al., 2006; Hutchings et al., 2009). The Lüderitz upwelling cell (~ 26° S) accounts for roughly 50 % of physical upwelling and separates the upwelling region into a northern and a southern subsystem (Shannon, 1985; Duncombe Rae, 2005). In the southern region (south of 26° S) the trade winds are seasonal and upwelling maximizes during austral spring and summer. The northern region (from 26° S to the ABFZ) is characterized by perennial alongshore winds and upwelling along the coast (Shannon, 1985).

The Lüderitz cell also marks the boundary of two central water regimes that cause distinct differences in biogeochemical properties of upwelling waters. Upwelling in the southern BUS entrains Eastern South Atlantic Central Water (ESACW) into the offshore Ekman drift (Duncombe Rae, 2005; Mohrholz et al., 2008). The ESACW is a central water mass that forms in the Indian Ocean and enters the South Atlantic Ocean by Agulhas Current intrusions (Poole and Tomczak, 1999; Stramma and England, 1999). Between the ABFZ and the Lüderitz cell, the ESACW mixes with an Angola Gyre subtype of the South Atlantic Central Water (SACW). This subtype of SACW originates in the subtropical Angola Gyre and enters the Namibian shelf and continental margin in a poleward undercurrent via the Angola Current (Duncombe Rae, 2005; Mohrholz et al., 2008). The SACW originally forms in the Brazil–Malvinas Confluence off South America (Gordon, 1981), flows eastward with the South Atlantic Current and is then diverted northwards along with the Benguela Current towards the equatorial current system. Here, a branch spreads eastwards and flows into the Angola Gyre (Poole and Tomczak, 1999). This Angola Gyre subtype is older and thus strongly enriched in nutrients and depleted in O₂ compared to the ESACW (Poole and Tomczak, 1999; Mohrholz et al., 2008). Increased inflow of SACW into the NBUS preconditions the development of an oxygen minimum zone (OMZ) and anoxic events over the Namibian shelf and upper slope (Weeks et al., 2002; Monteiro et al., 2006; Mohrholz et al., 2008).

On the shelf at low O₂ concentrations (< 20 µM O₂), fixed nitrogen (N) is reduced by denitrification and/or anammox (Lam and Kuypers, 2010; Kalvelage et al., 2011). The loss of fixed N to anammox within the OMZ on the shelf has been estimated to be ~ 1.4 Tg N yr⁻¹ (Kuypers et al., 2005) and the loss to denitrification to ~ 2.5 Tg N yr⁻¹ (Nagel et al., 2013). However, N loss exceeds estimates on N₂ fixation

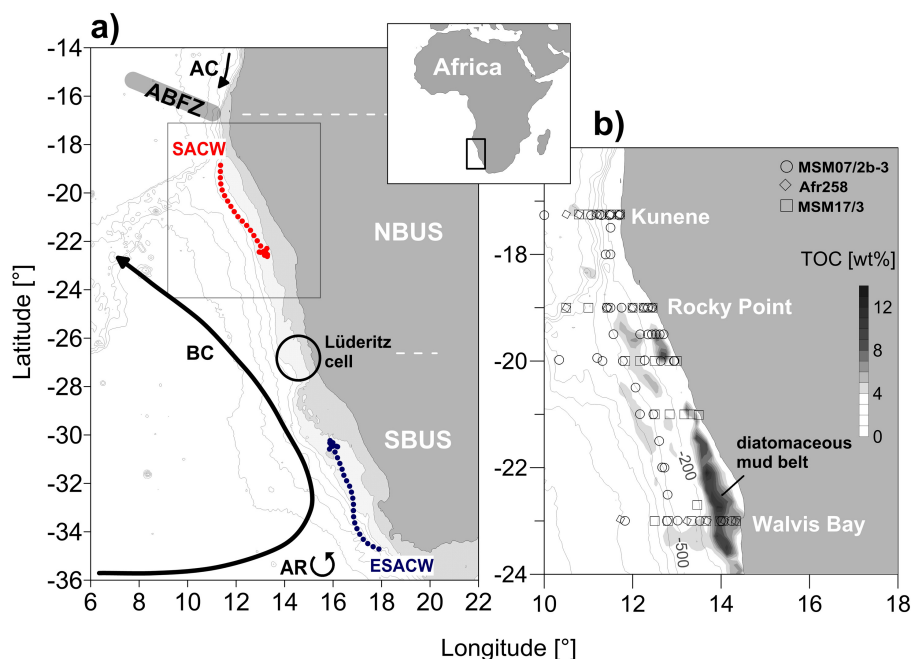


Fig. 1. (a) Schematic overview of the the Benguela upwelling system located at the southwestern coast of Africa. Surface currents are represented by solid lines and subsurface currents by dotted lines. AC, Angola Current; ABFZ, Angola Benguela Frontal Zone; AR, Agulhas rings; BC, Benguela Current; ESACW, Eastern South Atlantic Central Water; NBUS, northern Benguela upwelling system; SACW, South Atlantic Central Water; SBUS, southern Benguela upwelling system. (b) Stations sampled during the cruises: MSM07/2b-3 (circles), Afr258 (diamonds) and MSM17/3 (squares). The grey shading refers to the TOC content (wt %) of the surface sediments representing the diatomaceous mud belt (TOC data taken from Inthorn et al. (2006)/doi:10.1594/PANGAEA.351146).

(Sohm et al., 2011), suggesting that the BUS acts as net sink for fixed N. Furthermore, the BUS shelf is a region of modern phosphorite deposition (Glenn et al., 1994; Föllmi, 1996) associated with a massive organic-rich diatomaceous mud belt that roughly follows the Namibian coast between 50 and 200 m water depth (Fig. 1b) and covers an area of $\sim 18\,000\text{ km}^2$ (Bremner, 1980; Bremner and Willis, 1993; Emeis et al., 2004). The mud belt surface is settled by consortia of large sulfur bacteria (including *Thiomargarita namibiensis*) that release phosphate (P) into the anoxic pore water (Nathan et al., 1993; Schulz and Schulz, 2005; Goldhammer et al., 2010) and thereby enrich pore waters to $\sim 1000\text{ }\mu\text{M PO}_4^{3-}$ (van der Plas et al., 2007).

2.2 Water sampling, laboratory work and data analysis

Nutrient samples were collected during three cruises in austral summer and early autumn (Fig. 1b): MSM07/2b-3 (RV *Maria S. Merian*, 9 March–17 April 2008), Afr258 (RV *Africana*, 1–17 December 2009) and the MSM17/3 (RV *Maria S. Merian*, 31 January–8 March 2011). Sampled transects perpendicular to the coast stretched from the shelf, over the continental slope and into the open ocean. At least five stations per transect were sampled off Kunene (17.25° S), Rocky Point (19° S), Terrace Bay (20° S), Toscanini (20.80° S) and Walvis Bay (23° S). Transects off

Kunene, Rocky Point and Walvis Bay were sampled during all of the three cruises. Samples were collected by CTD casts using a rosette system equipped with 10 L Niskin bottles. The upper water column was sampled at fixed depth levels (5, 10, 15, 20, 30, 50, 100 and 200 m). From 200 m downwards the depth levels were extended to 100–300 m intervals depending on the bottom depth and, for example, the O_2 profile. The analysed parameters presented in this study comprise dissolved inorganic carbon (C_T), total alkalinity (A_T) and dissolved nutrients ($\text{NO}_x = \text{nitrate (NO}_3^-) + \text{nitrite (NO}_2^-)$ and phosphate (PO_4^{3-})). The apparent oxygen utilization (AOU) was calculated from O_2 concentrations using the equations for O_2 saturation according to Weiss (1970).

2.2.1 C_T and A_T

The C_T and A_T samples were taken during the MSM17/3 cruise. Transects off Kunene (17.25° S), Rocky Point (19° S), Terrace Bay (20° S), Toscanini (20.80° S) and Walvis Bay (23° S) were sampled. For C_T and A_T analysis the samples were filled into 250 mL borosilicate bottles using silicone tubes (Tygon). The bottles were rinsed twice and filled from the bottom to avoid air bubbles. Duplicate samples were periodically taken. The samples were fixed with mercury (II) chloride solution (250 μL of a 35 g L^{-1} HgCl_2 solution) directly after collection and analysed on board using

the VINDTA 3C system (Mintrop, 2005). The A_T was determined on the basis of a semi-closed cell titration principle. The samples were titrated with a fixed volume of hydrochloric acid (HCl, 0.1 N). C_T was quantified by the coulometric method (Coulometer CM 5015, precision of 0.1 %) after extracting the CO_2 out of the acidified water samples. Certified reference material (CRM, batch #101 and #104, provided by A. Dickson (Scripps Institution of Oceanography, La Jolla, CA, USA)) was used to calibrate the VINDTA 3C system. Measured A_T and C_T values agreed within $\pm 2.5 \mu\text{mol kg}^{-1}$ for the CRMs and within $\pm 2 \mu\text{mol kg}^{-1}$ for the duplicate samples. In the following A_T is reported as the salinity corrected value ($A_T = A_{T\text{meas}} \times 35/S_{\text{meas}}$).

2.2.2 Dissolved nutrients

The nutrient samples were filtered through disposable syringe filters (0.45 μm) immediately after sampling, filled into prerinsed 50 mL PE bottles and frozen (-20°C). Samples collected during the MSM07/2b-3 cruise were measured on board, whereas samples taken during Afr258 and MSM17/3 cruises were analysed in the shore-based laboratory subsequent to the expedition. Dissolved nutrients were measured by a continuous-flow injection system (Skalar SAN plus System) according to methods described by Grasshoff et al. (1999). The detection limits were $\text{NO}_x = 0.08 \mu\text{M}$ and $\text{PO}_4^{3-} = 0.07 \mu\text{M}$ according to DIN 32645. Ammonium (NH_4^+) concentrations were usually $< 2.5 \mu\text{mol kg}^{-1}$ and are not discussed in this paper. In the following N = nitrate (NO_3^-) + nitrite (NO_2^-) and P = PO_4^{3-} will be used throughout the paper.

2.2.3 Elemental stoichiometry

To calculate the deviation from the classical Redfield ratio (N : P = 16 : 1) (Redfield et al., 1963), we used the tracer N^* (Gruber and Sarmiento, 1997):

$$N^* = ([\text{NO}_3^-] - 16 \cdot [\text{PO}_4^{3-}] + 2.9) \cdot 0.87, \quad (1)$$

where $[\text{NO}_3^-]$ and $[\text{PO}_4^{3-}]$ are the concentrations of nitrate and phosphate in $\mu\text{mol kg}^{-1}$, respectively. The constants drive the global mean N^* value of $-2.9 \mu\text{mol kg}^{-1}$ to zero. Positive and negative N^* are indicative of an excess and deficit of NO_3^- relative to PO_4^{3-} , respectively (Gruber and Sarmiento, 1997). To quantify the PO_4^{3-} anomaly (P^*) from Redfield we use the concept of Deutsch et al. (2007):

$$P^* = [\text{PO}_4^{3-}] - [\text{NO}_3^-]/16. \quad (2)$$

N^* and P^* are a measure for the deviation from the Redfield ratio and are arbitrary values rather than definite concentrations.

2.3 Characterization of central water masses

The potential temperature (T_{pot}) and salinity (S) characteristics were used to differentiate between SACW and ESACW

contributions. Their definitions were adopted from Mohrholz et al. (2008), who identified an Angola Gyre subtype of SACW. This subtype is characterized by O_2 concentrations ranging between 22 and $68 \mu\text{mol L}^{-1}$ in contrast to the ESACW that shows O_2 values of 249–300 $\mu\text{mol L}^{-1}$ in the Cape Basin (Poole and Tomczak, 1999; Mohrholz et al., 2008). The SACW and ESACW are defined by a line in $T_{\text{pot}} - S$ space that can be described by the following equations:

$$T_{\text{potESACW}} = 9.4454 \cdot S_{\text{ESACW}} - 319.03, \quad (3)$$

$$T_{\text{potSACW}} = 8.5607 \cdot S_{\text{SACW}} - 289.08. \quad (4)$$

The above equations were transformed to calculate the respective proportions of SACW and ESACW:

$$S_{\text{SACW}} = (T_{\text{pot}} + 289.08)/8.5607, \quad (5)$$

$$S_{\text{ESACW}} = (T_{\text{pot}} + 319.03)/9.4454, \quad (6)$$

$$S_{\text{measured}} = a \cdot S_{\text{SACW}} + b \cdot S_{\text{ESACW}}, \text{ whereby } a + db = 1 \quad (7)$$

Data derived from water depths above 100 m were excluded from this mixing analysis due to the non-conservative behaviour of T_{pot} and S at shallow water depths. The relative contributions are reported in percentage (%). The $T_{\text{pot}} - S$ range used to calculate the relative contribution of SACW and ESACW is shown in Fig. 2 for the example of the MSM17/3 cruise.

3 Results and discussion

On a global scale the distribution of N : P is characterized by a deficit of N towards P with regard to the Redfield ratio (Gruber and Sarmiento, 1997; Tyrrell and Law, 1997). The loss of fixed N is caused by heterotrophic denitrification and anammox occurring in the oceanic OMZs (Lam and Kuypers, 2010) but also in shallow coastal OMZs, for example on the Namibian shelf. Here, N loss (Kuypers et al., 2005; Nagel et al., 2013) along with the accumulation of P in sub- and anoxic bottom waters (Goldammer et al., 2010) result in extremely low N : P ratios in the water column. In the following the C : N : P : $-\text{O}_2$ remineralization patterns observed in 2011 are discussed with regard to their spatial variability and are complemented by results on the temporal variability of N : P anomalies recorded in 2008 and 2009.

3.1 C : N : P : AOU stoichiometry

The N and P concentrations of the NBUS scatter to both sides of the reference Redfield slope and characterize the NBUS

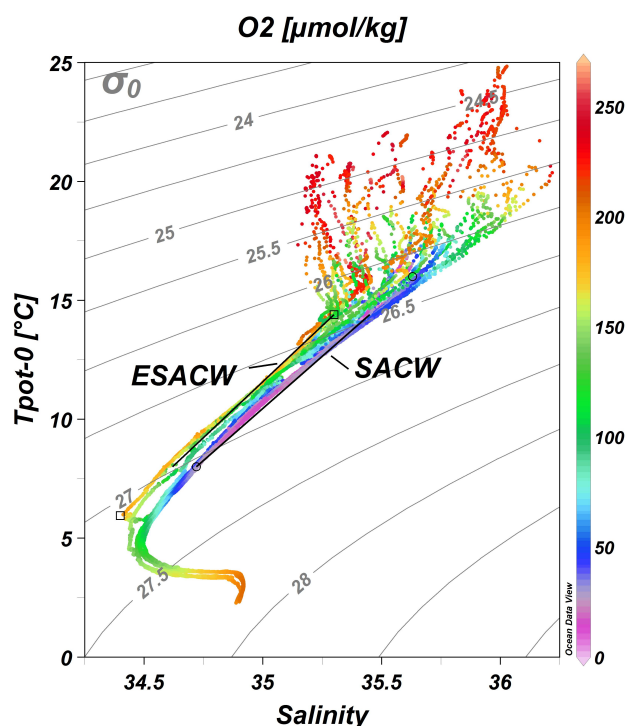


Fig. 2. $T_{\text{pot}} - S$ diagram of vertical water column profiles measured in the NBUS region during the MSM17/3 cruise. The O_2 concentration ($\mu\text{mol kg}^{-1}$) is indicated by coloured shading, and isopycnals (kg m^{-3}) are given by the grey lines. The end points of Eastern South Atlantic Central Water (ESACW, open squares) and South Atlantic Central Water (SACW, open circles) specify the definition source water types given in the text. The $T_{\text{pot}} - S$ range used to calculate their relative contribution in water samples from >100 m depth is indicated by the black lines.

as a system that produces both positive and negative deviations from Redfield ratio expressed in positive and negative N^* anomalies (Fig. 3). Major negative anomalies were apparent at shelf sites. Tyrrell and Lucas (2002) attributed low N:P (LNP) data ($\text{N}:\text{P} < 3$ and $\text{P} > 1.5 \mu\text{mol kg}^{-1}$) in waters of the BUS to nutrient trapping and denitrification that leads to a relative accumulation of P. Figure 4 illustrates the relationships between apparent oxygen utilization (AOU), N, P, A_T and C_T of the water samples in 2011 (MSM17/3). The observed average C_T : AOU ratio of 0.76 ($r^2 = 0.89$) is close to that expected from a mineralization C : $-\text{O}_2$ ratio of 106 : -138 (Fig. 4a). Exclusion of the $\text{O}_2 < 20 \mu\text{mol kg}^{-1}$ data gave no mentionable differences between the shelf (C_T : AOU = 0.77, $r^2 = 0.88$) and offshore sites (C_T : AOU = 0.75, $r^2 = 0.89$). The scattering of the data in Fig. 4a is likely due to the fact that the shelf system is not truly closed and that O_2 is introduced into the subsurface water masses on the shelf through mixing (Ito et al., 2004). The increase of C_T at AOU $> 230 \mu\text{mol kg}^{-1}$ corresponding to $\text{O}_2 < 20 \mu\text{mol kg}^{-1}$ implies C_T input from anaerobic respiration, such as denitrification, and is evident

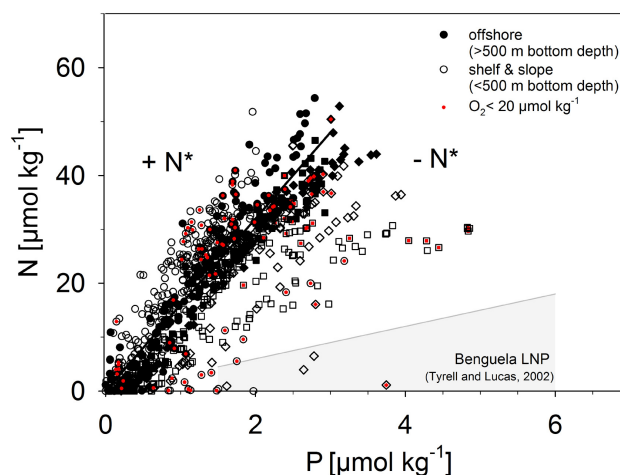


Fig. 3. Composite of N versus P ($\mu\text{mol kg}^{-1}$) data of the MSM07/2b-3 cruise (circles), Afr258 cruise (diamonds) and MSM17/3 cruise (squares). The data were separated into shelf and slope stations (< 500 m bottom depth), indicated by open symbols, and offshore stations (> 500 m bottom depth), indicated by black-filled symbols. The red-filled symbols correspond to data points associated with $\text{O}_2 \leq 20 \mu\text{mol kg}^{-1}$. Positive and negative deviations from the expected N : P correlation of 16 : 1 (black line) are expressed in $+N^*$ and $-N^*$ (Gruber and Sarmiento, 1997). The grey-shaded area refers to the range of low N : P (LNP) defined by Tyrrell and Lucas (2002).

from decreasing N associated with increasing C_T concentrations (Fig. 4b). At O_2 concentrations $< 20 \mu\text{mol kg}^{-1}$, both anammox and denitrification increased A_T through the consumption of N (Fig. 4d). However, a decrease in C_T indicating a dominance of anammox over heterotrophic denitrification is not visible in our data (Fig. 4b), likely due to the low C : N stoichiometry of anammox ($\text{C}:\text{N} \sim -0.07 : -1.3$) compared to that of denitrification ($\text{C}:\text{N} \sim 106 : -104$) (Koeve and Kähler, 2010). A loss of N by $20 \mu\text{mol kg}^{-1}$ would result in a C_T decrease of $-1 \mu\text{mol kg}^{-1}$ due to anammox and a C_T increase of $+21 \mu\text{mol kg}^{-1}$ during denitrification. At higher O_2 the overall average C_T : N = 6.1 ($r^2 = 0.86$) is similar to the Redfield ratio of 6.6, with slightly lower values in the open ocean (5.5, $r^2 = 0.89$) than on the shelf (6.8, $r^2 = 0.86$). The slope of A_T : $C_T \sim -0.15$ (Fig. 4d) observed in the paired data with $> 20 \mu\text{mol kg}^{-1}$ O_2 agrees with the expected effect of aerobic organic matter remineralization (A_T : $C_T = -16 : 106$) (Broecker and Peng, 1982) and implies that carbonate dissolution hardly affected the C_T and A_T concentrations.

A source of P besides the mineralization of organic matter in the water column is suggested by the spread of the C_T : P data in Fig. 4c. Open-ocean sites had an average C_T : P ratio of 101 : 1, which is similar to the global mean C : P ratio of 106 : 1 (Redfield et al., 1963; Anderson and Sarmiento, 1994). The C_T : P correlation of the shelf data splits in two groups. One group reveals a slope of the regression line of

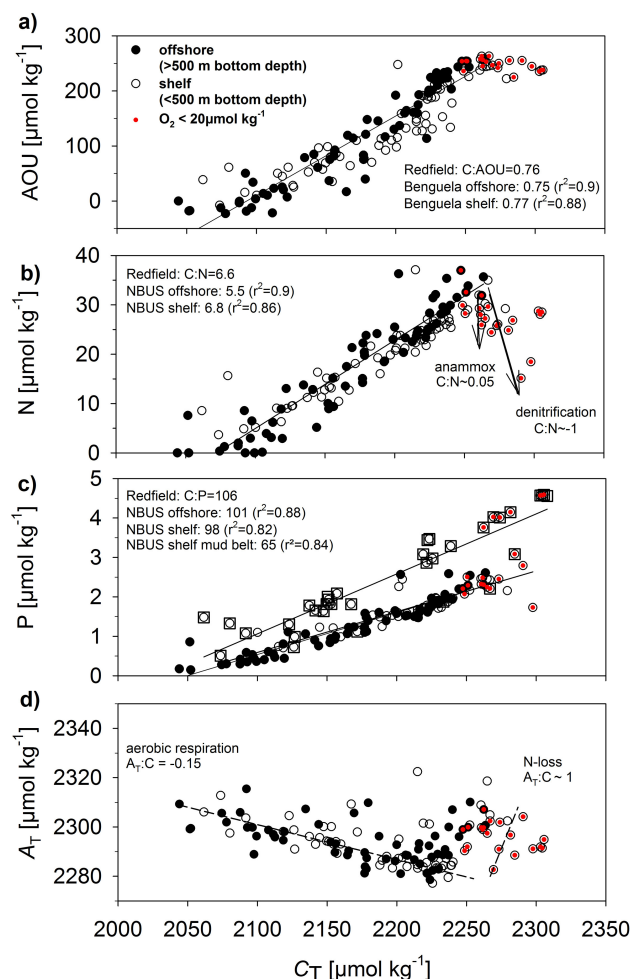


Fig. 4. (a) AOU, (b) N, (c) P and (d) A_T versus C_T (all in $\mu\text{mol kg}^{-1}$) as measured within the range of 30–500 m water depth during the MSM17/3 cruise. The data were separated into shelf stations (<500 m bottom depth, open circles) and offshore stations (>500 m bottom depth, black circles). The red-filled symbols correspond to data points associated with O_2 concentrations $\leq 20 \mu\text{mol kg}^{-1}$. The correlations observed for the Benguela are given and indicated by the black line. The reported ratios in panel (a) and (b) are derived by excluding the $\leq 20 \mu\text{mol kg}^{-1}$ data. The open squares in panel (c) represent data from the mud belt region. (d) The dashed black lines indicate the expected correlation caused by aerobic mineralization $A_T:C = -16:106 = -0.15$ (Redfield et al., 1963) and N loss, e.g. due to denitrification $A_T:C = 104:106 \sim 1$ (Gruber and Sarmiento, 1997).

$\sim 98:1$ ($r^2 = 0.82$) that is slightly lower but similar to those seen in the offshore samples. The remaining samples suggest a much lower average $C_T:P$ ratio of ~ 65 ($r^2 = 0.84$) and are related to the mud belt region, where even lower C:P ratios of 33–48 were measured in pore waters near the sediment–water interface (Goldammer et al., 2011). The low $C_T:P$ occurring exclusively at shelf sites indicate an impact of pore water P effluxes from the anoxic mud sediments mediated by

consortia of sulfur bacteria (Schulz and Schulz, 2005). This is in line with previous hypotheses that the stoichiometric N deficit in waters over the Namibian shelf is, in addition to the impact of N reduction, in part caused by P fluxes across the sediment–water interface (Bailey and Chapman, 1991; Nagel et al., 2013). Accordingly, the impact of N loss and benthic P fluxes on the suboxic bottom layer should be observable by a spatial decoupling of the N and P maxima; that is, N_{max} would be expectable outside the OMZ, while P_{max} would be expectable inside the OMZ. This is in agreement with our observations of N and P maxima along the Namibian shelf and slope (Fig. 5, MSM17/3 cruise in February 2011). The OMZ was positioned between 300 and 400 m water depth off Kunene (17.25°S) (Fig. 5a), stretching from the slope towards the open ocean. The maxima of N ($45 \mu\text{mol kg}^{-1}$) and P ($2.8 \mu\text{mol kg}^{-1}$) were observed at the same depth ranges slightly below the OMZ. In contrast, the OMZ was restricted to the shallow shelf region off Walvis Bay (23°S) (Fig. 5b) overlying the diatomaceous mud belt, where the large sulfur bacteria occur that release P into the anoxic pore water (Goldammer et al., 2011). In fact, P_{max} was strongly elevated ($4.8 \mu\text{mol kg}^{-1}$), and coincided with the OMZ, while N_{max} had decreased to $35 \mu\text{mol kg}^{-1}$ and was observed outside the OMZ. This increase of P relative to N is reflected in a pronounced N:P deviation from Redfield, as indicated by strongly decreased N^* values over the shelf and shelf break off Walvis Bay (23°S) compared to Kunene (17.25°S). Although the N loss likely contributes to the overall N decrease, it also reflects the gradual increase of the ESACW fraction towards the south. This water mass is characterized by lower nutrient concentrations than SACW (Poole and Tomczak, 1999; Mohrholz et al., 2008).

To summarize, C:N:P: $-O_2$ ratios at offshore sites are 101:16:1:138 and are close to Redfield ratios. Over the Namibian shelf, with particular regard to the mud belt region, increased P concentrations result in a C:N:P: $-O_2$ ratio of 106:16:1.6:138. In regions with O_2 concentrations $< 20 \mu\text{mol kg}^{-1}$, denitrification further increases C:N and denitrification along with anammox further lower N:P ratios.

3.2 Spatial and temporal variability

Inter-annual differences in upwelling conditions during austral summer expeditions were well reflected in the distribution of sea surface temperatures (SST). The SST patterns, measured continuously by thermo-salinographs at 5 m water depth, indicate that upwelling was most intense in December 2009 (Afr258) (Fig. 6), when minimum SST (15°C) occurred along the entire coast and temperatures $< 20^\circ \text{C}$ were measured far offshore. In contrast, most of the NBUS had SST $> 20^\circ \text{C}$ during February 2011 (MSM17/3). In March 2008 (MSM07/2b-3) SSTs outline an intermediate upwelling intensity in a coastal band of low temperatures. Stronger or weaker upwelling is also associated with

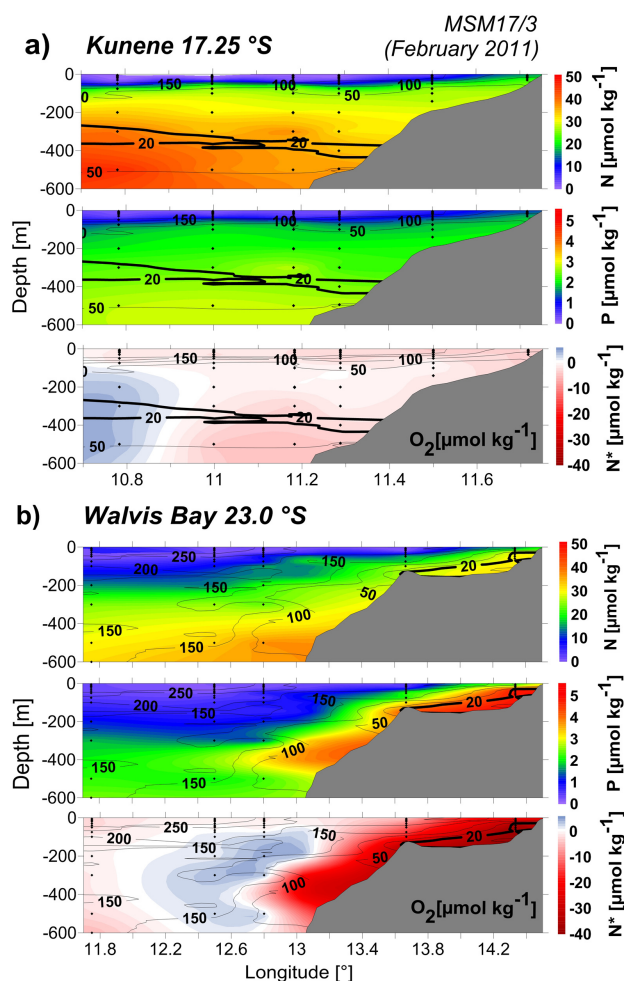


Fig. 5. Cross-shelf transects off (a) Kunene (17.25° S) and (b) Walvis Bay (23.0° S) during MSM17/3 cruise showing the spatial decoupling of N and P maxima expressed in N^* . The N, P and N^* concentrations (coloured shading, in $\mu\text{mol kg}^{-1}$) are overlain by the O_2 concentrations (contoured at $50 \mu\text{mol kg}^{-1}$ intervals, black isolines). The area of low O_2 concentration ($\leq 20 \mu\text{mol kg}^{-1}$) is marked by the bold black line. The sampled stations used for gridding are indicated by black circles; areas of no data were extrapolated (kriging method).

distinct distributions of the central water masses on the shelf. Mohrholz et al. (2008) found that vigorous cross-shelf circulation during phases of strong upwelling suppresses the along-shelf poleward undercurrent of SACW from the north. Weak upwelling phases, such as that in February 2011, permit SACW to protrude far southward as indicated by the high SACW contribution (70 %) off Walvis Bay (23° S) (Fig. 7d–f). SACW is characterized by much lower O_2 concentrations than ESACW (Mohrholz et al., 2008), which is also evident from our data (Fig. 2). In fact, the dominance of SACW was reflected in mid-water O_2 deficits, and thus samples with ≥ 80 % SACW were associated with $\leq 50 \mu\text{mol kg}^{-1}$ O_2 (Fig. 7). However, during strong and weak upwelling alike,

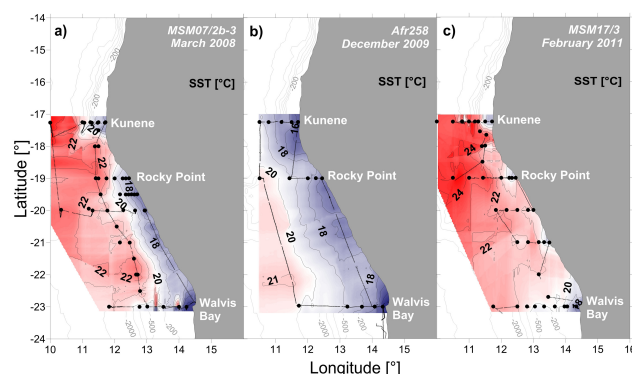


Fig. 6. Distribution of sea surface temperature (SST) (contoured at 1 °C intervals) at 5 m depth continuously measured along the cruise track during (a) MSM07/2b-3, (b) Afr258 and (c) MSM17/3. Sampled stations (black circles) and cruise track (black line) were used for gridding; areas of no data were extrapolated (kriging method).

and regardless of the SACW contribution, the O_2 concentrations on the shelf off Walvis Bay were $< 20 \mu\text{mol kg}^{-1}$ during all cruises. This reflects the strong O_2 demand caused by the organic-rich mud belt area and is in line with previous studies showing that SACW sets the precondition for anoxia in bottom waters off Walvis Bay but that the local sedimentary O_2 demand plays a decisive role as well (Monteiro et al., 2006; van der Plas et al., 2007).

The N : P deviation from Redfield varied during the different expeditions and upwelling states (Fig. 8). Pronounced negative N^* concentrations were observed in coastal bottom waters, in particular off Rocky Point and Walvis Bay (Fig. 8a–c), and are comparable with reported values (Tyrrell and Lucas, 2002; Nagel et al., 2013). Elevated N^* was observed at offshore sites and differed strongly in magnitude especially offshore of Kunene (17.25° S), where SACW dominates (Fig. 7d–f), indicating that the N^* signature of SACW differs. From the temporal variability of N^* in the hemipelagic OMZ offshore of Kunene, it is apparent that N^* in the SACW water mass varied significantly between years (Fig. 9). During March 2008 (MSM07/2b-3), N^* had increased threefold within the OMZ ($N^* \sim 12 \mu\text{mol kg}^{-1}$) compared to December 2009 and February 2011 ($N^* \sim 3$ – $4 \mu\text{mol kg}^{-1}$). This positive N^* anomaly was imported to the NBUS in 2008 along with SACW, and thus water masses on the shelf were less N^* -deficient (Fig. 8a–c) despite similarly low O_2 concentrations in 2009 and 2011 (Fig. 7a–c). Strong local sedimentary O_2 demand caused by the organic-rich mud belt area (Fig. 1b) is suggested by low N^* observed, for example, off Rocky Point in 2008 despite high SACW contribution (Figs. 7 and 8a). In contrast to the situation in March 2008 (MSM07/2b-3), most of the NBUS area revealed negative N^* concentrations in December 2009 (Afr258) and February 2011 (MSM17/3), and strongest N^* deficits ($N^* \sim -35 \mu\text{mol kg}^{-1}$) off Walvis Bay exceeded the N^* deficits

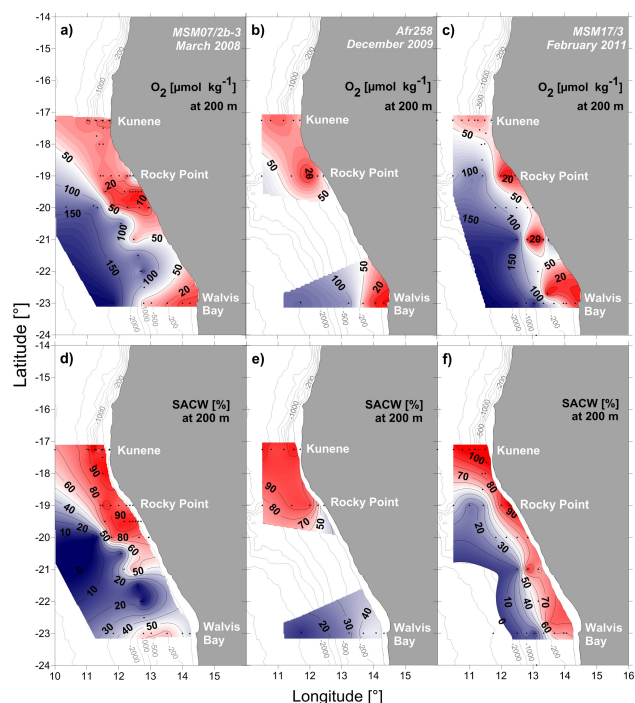


Fig. 7. (a–c) Distribution of O_2 ($\mu\text{mol kg}^{-1}$) and (d–f) contribution of SACW and ESACW (%) at 200 m water depth. Note: shelf stations with bottom depths shallower than 200 m were included in the O_2 interpolation and stations with bottom depths deeper than 100 m were included in the SACW interpolation. The sampled stations used for gridding are marked by black circles; areas of no data were extrapolated (kriging method). Zero percent SACW is equivalent to 100 % ESACW.

in March 2008 by a factor of >2 . The results suggest that the considerable variability in nutrient ratios of SACW controls the inter-annual variability of N^* in the NBUS. The impact of ESACW entering the NBUS from the south is difficult to assess from our data due to a lack of ESACW samples from the southern BUS. The ESACW sampled in the NBUS is characterized by lower O_2 concentrations (~ 150 – $200 \mu\text{mol kg}^{-1}$) (Fig. 2) than reported for ESACW from the southern BUS region (250 – $300 \mu\text{mol L}^{-1}$) (Poole and Tomczak, 1999), indicating that ESACW is modified by aerobic mineralization on its way from the SBUS to the NBUS region. Following the nutrient signature of ESACW given by Poole and Tomczak (1999), N^* ranges between -5.45 and $-0.762 \mu\text{mol L}^{-1}$. Assuming mineralization according to the Redfield stoichiometry under these oxygenated conditions and further assuming the absence of N_2 fixation in the SBUS implies that the N^* signature of ESACW should not be further altered on its way towards the NBUS. An intrusion of ESACW would therefore instead contribute to the negative N^* signal observed over the NBUS shelf. However, off the western South African coast, N^* was shown to vary between 0 and $5 \mu\text{mol kg}^{-1}$ along the $\sigma_\theta = 26.50$ and 27.1 kg m^{-3} surfaces (Gruber and Sarmiento, 1997), referring to a depth

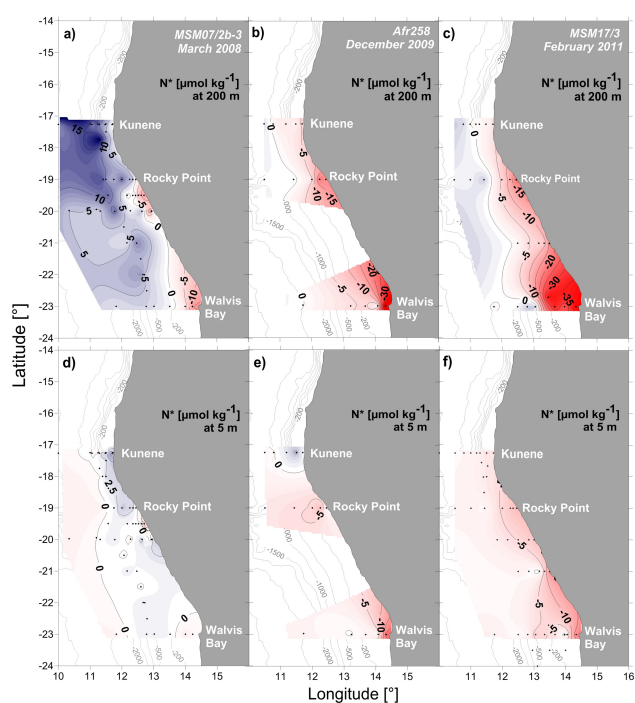


Fig. 8. Distribution of N^* ($\mu\text{mol kg}^{-1}$) (a–c) at 200 m and (d–f) at 5 m water depth (contoured at $5 \mu\text{mol kg}^{-1}$ intervals). Note: shelf stations with bottom depths shallower than 200 m were included in the N^* interpolation. The sampled stations used for gridding are marked by black circles; areas of no data were extrapolated (kriging method).

range where ESACW occurs. This suggests that, comparable to SACW, the N^* signature in ESACW might vary; however this aspect is not further addressed owing to the low density of ESACW data.

Positive N^* anomalies in subsurface waters are commonly attributed to the mineralization of organic matter produced by N_2 -fixing organisms (Gruber and Sarmiento, 1997) that have $N:P$ ratios of up to 150 (Krauk et al., 2006). The impact of mineralization is reflected in minimum O_2 concentrations that coincided with maximum N^* values within the SACW fraction (Fig. 9). Positive N^* anomalies in the tropical and subtropical North Atlantic are $\sim 4 \mu\text{mol kg}^{-1}$ at $\sigma_\theta = 26.5 \text{ kg m}^{-3}$ (Gruber and Sarmiento, 1997; Mahaffey et al., 2005). Here, intensive blooms of *Trichodesmium* spp. (Carpenter, 1983; Tyrrell et al., 2003; Capone et al., 2005) and high $N:P$ (of up to 35) have been reported (Mahaffey et al., 2003) and are consistent with N_2 fixation as a significant input source, which can raise N^* to $\sim 20 \mu\text{mol kg}^{-1}$ (Mahaffey et al., 2003). In contrast, the South Atlantic Gyre has low positive N^* (Gruber and Sarmiento, 1997), in line with low rates of N_2 fixation (Mahaffey et al., 2005). N_2 fixation is facilitated by P and the availability of micronutrients, e.g. iron (Fe) (Mills et al., 2004). The low N_2 fixation in the South Atlantic has been attributed to a lack of Fe supply rather

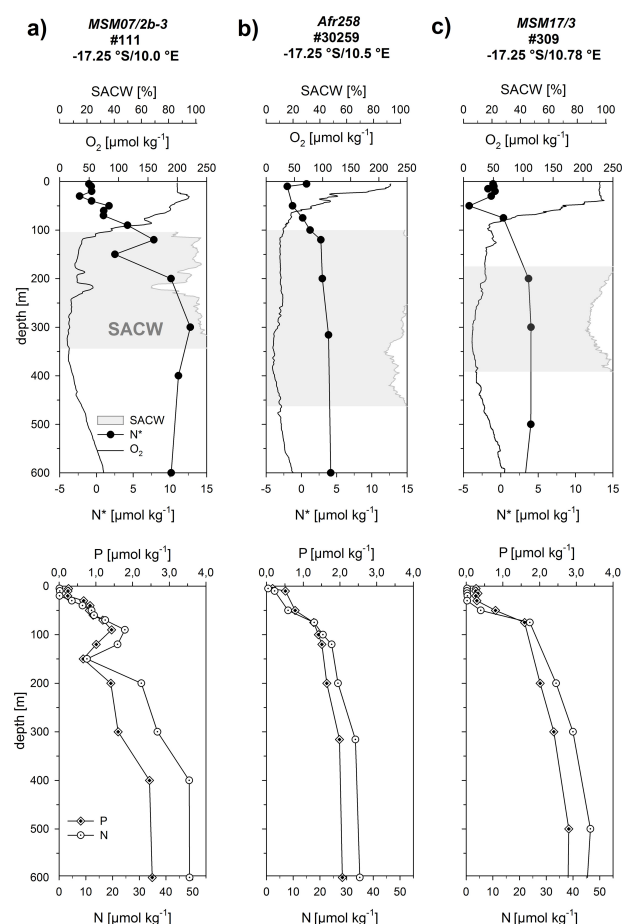


Fig. 9. Vertical profiles of SACW (%), O_2 , N^* , P and N (all in $\mu\text{mol kg}^{-1}$) during (a) MSM07/2b-3, (b) Afr258 and (c) MSM17/3 at offshore stations with comparable location offshore of Kunene (17.25°S). The contribution of SACW is indicated by the grey shading.

than P availability (Moore et al., 2009). This is supported by the negative N^* observed in the surface water offshore of Kunene (Fig. 9) caused by P concentrations that ranged between 0.17 and $0.28 \mu\text{mol kg}^{-1}$ and exceeded N concentrations, resulting in surface water N^* deficits. The very low N concentrations further suggest that atmospheric deposition that is assumed to be another significant N source to the ocean (Duce et al., 2008; Baker et al., 2013) is negligible. However, Sohm et al. (2011) observed N_2 fixation within the ABFZ (~ 13 – 15°S) coinciding with decreased thermocline $\delta^{15}\text{N}_{\text{NO}_3^-}$ values and elevated dissolved Fe and cobalt surface concentrations (Noble et al., 2012), which are important micronutrients for marine diazotrophic cyanobacteria (Saito et al., 2002, 2004). The studies of Sohm et al. (2011) and Noble et al. (2012) were performed from November to December 2007 and hence ~ 4 months prior to the MSM07/2b-3 expedition in March 2008 that found the positive N^* anomaly in SACW. This time period is comparable to the time lag

of ~ 2 months that was observed between the occurrence of *Trichodesmium* spp. and the response in N^* (Singh et al., 2013). Although the N_2 fixation rates were relatively low (22 – $85 \mu\text{mol N m}^{-2} \text{d}^{-1}$) (Sohm et al., 2011), it was proven that N_2 fixation occurs north of the ABFZ, even with high nitrate concentrations ($\sim 20 \mu\text{mol L}^{-1}$) in surface water. This finding seems to challenge the traditional paradigm of high N_2 fixation activity being restricted to oligotrophic regions. However, there is growing evidence based on laboratory and field studies showing that N_2 fixation occurs under nutrient-rich conditions (Sohm et al., 2011; Knapp, 2012; Knapp et al., 2012; Subramaniam et al., 2013). It suggests that Fe might be the factor limiting N_2 fixation at the ABFZ. In contrast to the Sahara dust plumes influencing the North Atlantic, the eastern South Atlantic experiences much lower aeolian input (Jickells et al., 2005; Mahowald et al., 2009). Dust plumes off Namibia are channelled by dry river beds and appear to be much more restricted to near-shore regions (Eckardt and Kuring, 2005). However, dust transport from southern Africa to the South Atlantic has been reported for austral spring (Swap et al., 1996; Sarthou et al., 2003), further supported by Tyson et al. (1996), who found that the main air mass transport to the South Atlantic peaks during austral spring and summer, indicating that N_2 fixation initiated by atmospheric Fe input is expectable during this time of the year, in line with the results of Sohm et al. (2011). Although not as pronounced as in March 2008, N^* was also elevated during December 2009 and February 2011 within the SACW fraction, suggesting that N_2 fixation is apparent albeit of lower magnitude. Alternatively to atmospheric Fe sources, hypoxic bottom waters of the Angolan and Namibian shelf reveal high concentrations of dissolved and particulate Fe (Bowie et al., 2002; Noble et al., 2012). It suggests that upwelling of these bottom waters along the Angolan and Namibian coast serves as an Fe source analogue to the California and Peru upwelling system (Johnson et al., 2001; Bruand et al., 2005). In view of the findings on diazotrophy under nutrient-rich conditions, we assume that N_2 fixation is a feasible input source that caused the observed N excess in the SACW in 2008. Furthermore, methodological improvements (Mohr et al., 2010; Großkopf et al., 2012) and the broadening range of identified species involved in N_2 fixation (Moisander et al., 2010; Zehr, 2011) suggest that rates and regions of N_2 fixation may have been considerably underestimated so far.

3.3 NBUS – a P^* source for the South Atlantic

Upwelling of N-deficient water in 2009 and 2011 caused lowest N^* at 5 m depth close to the coast (Fig. 8d–f), indicating that a relative P surplus surfaces and is advected offshore into the open ocean with modified upwelling water. This should stimulate N_2 fixation in the adjacent hemipelagic ocean (Deutsch et al., 2007), but experimentally determined rates of N_2 fixation in the NBUS were very low to not

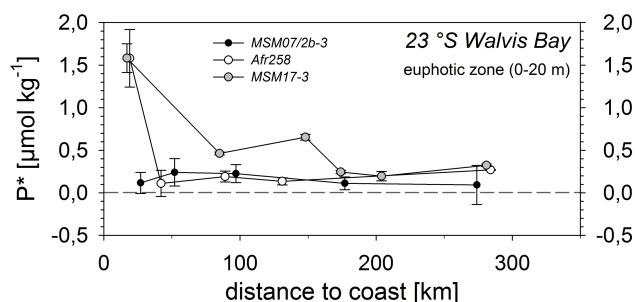


Fig. 10. Averaged P^* ($\mu\text{mol kg}^{-1}$) of the euphotic zone (0–20 m) versus distance to the coast (km) during MSM07/2b-3 (black circles), Afr258 (open circles) and MSM17/3 (grey circles) along the Walvis Bay transect (23°S).

detectable (N. Wasmund, personal communication, 2012). We calculated the P excess (P^*) within the euphotic zone (0–20 m) that is exported offshore for the Walvis Bay (23°S) transect (Fig. 10). Roughly 300 km offshore, beyond the continental slope, P^* was close to zero in March 2008 ($P^* = 0.007 \pm 0.09 \mu\text{mol kg}^{-1}$), suggesting that the NBUS at that time was not a regional source of P for the oligotrophic subtropical South Atlantic. During the other cruises, the NBUS was a relative P source, with P^* values of $0.3 \pm 0.01 \mu\text{mol kg}^{-1}$. These observations are in line with Staal et al. (2007) and Moore et al. (2009), who reported surface $P^* = 0.15\text{--}0.30 \mu\text{mol kg}^{-1}$ within areas of the subtropical gyre that are influenced by the advection of water masses transported by the Benguela Current. Along with our findings, this implies that the coastal upwelling system over the shelf is a P^* source to the South Atlantic most of the time. As shown before, the bottom water off Walvis Bay was low in O_2 , independent of the upwelling situation (Fig. 8), leading to strongly elevated P and reduced N maxima off Walvis Bay (Fig. 5). This implies that especially the mud belt of the shallow central Namibian shelf is a region of continuous $+P^*$ generation via N loss and P efflux. We assume that the inter-annual variability of P^* in the surface (Fig. 10) depends mainly on the magnitude of $+N^*$ in the SACW that is likely produced by N_2 fixation north of the ABFZ. We further presume that N_2 fixation in this region is in turn linked to the NBUS by the export of $+P^*$ into the South Atlantic Ocean and its advection along with the major surface currents to the Angola Gyre and ABFZ region (Fig. 11).

4 Conclusions

Our data measured during the cruise in March 2011 show a mean C:N:P:– O_2 ratio that is close to the Redfield stoichiometry. Over the mud belt of the Namibian shelf, pore water fluxes lowered the C:N:P:– O_2 ratio to 106:16:1.6:138. N losses further increased C:N and decreased N:P ratios in restricted regions where O_2 concentra-

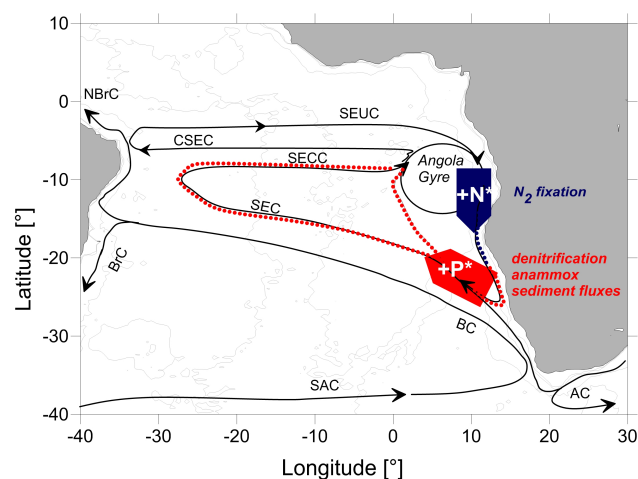


Fig. 11. Map of the wind-driven large-scale circulation (upper 100 m) of the South Atlantic Ocean adapted from Stramma and England (1999). The map illustrates the hypothetical advection of $+P^*$ (red dashed line) via SEC and SECC towards the Angola Gyre, where it fuels N_2 fixation and in turn results in $+N^*$ (blue dashed line) that is introduced into the NBUS. AC, Agulhas Current; BC, Benguela Current; BrC, Brazil Current; CSEC, central South Equatorial Current; NBrC, North Brazil Current; SAC, South Atlantic Current; SEC, South Equatorial Current; SECC, South Equatorial Countercurrent; and SEUC, South Equatorial Undercurrent.

tions dropped below $20 \mu\text{mol kg}^{-1}$. Additional nutrient data measured during two cruises in 2008 and 2009 reveal an inter-annual variability of N excess within the SACW that flows from the north into the NBUS with highest N^* values observed in 2008. The degree to which the N loss on the shelf is balanced by enhanced inputs of N along with the SACW controls the amount of P^* that is exported from the NBUS into the subtropical South Atlantic. To better understand the role of the northern Benguela upwelling system as P source and N sink, factors controlling the occurrence of N_2 fixation at the Angola Benguela Frontal Zone need to be addressed in future studies.

Acknowledgements. We would like to thank all scientists, technicians, captains and crews on board the research vessels RV *Africana* and RV *Maria S. Merian*. M. Birkicht is acknowledged for the nutrient analysis. We sincerely thank L. Lehnhoff and C. G. Steigüßer for their help during and subsequent to the expeditions. S. Christof and N. Moroff are thanked for their comprehensive support during the stay in Swakopmund. The comments made by three reviewers have helped in improving the final version of the paper and are gratefully acknowledged. Furthermore, we are grateful to the German Federal Ministry of Education and Research (BMBF) for financial support of the GENUS project (03F0497D – ZMT).

Edited by: M. Dai

References

- Anderson, L. A. and Sarmiento, J. L.: Redfield ratios of remineralization determined by nutrient data analysis, *Global Biogeochem. Cy.*, 8, 65–80, 1994.
- Arrigo, K. R.: Marine microorganisms and global nutrient cycles, *Nature*, 437, 349–355, doi:10.1038/nature04158, 2005.
- Bailey, G. W. and Chapman, P.: Short-term variability during an anchor study in the southern Benguela upwelling system: chemical and physical oceanography, *Oceanogr.*, 28, 9–37, 1991.
- Baker, A. R., Adams, C., Bell, T. G., Jickells, T. D., and Ganzeveld, L.: Estimation of atmospheric nutrient inputs to the Atlantic Ocean from 50° N to 50° S based on large-scale field sampling: Iron and other dust-associated elements, *Global Biogeochem. Cy.*, 27, 755–767, doi:10.1002/gbc.20062, 2013.
- Behrenfeld, M. J., O'Malley, R. T., Siegel, D. A., McClain, C. R., Sarmiento, J. L., Feldman, G. C., Milligan, A. J., Falkowski, P. G., Letelier, R. M., and Boss, E. S.: Climate-driven trends in contemporary ocean productivity, *Nature*, 444, 752–755, doi:10.1038/nature05317, 2006a.
- Behrenfeld, M. J., Worthington, K., Sherrell, R., Chavez, F. P., Strutton, P., McPhaden, M., and Shea, M. D.: Controls on tropical Pacific Ocean productivity revealed through nutrient stress analysis, *Nature*, 442, 1025–1028, doi:10.1038/nature05083, 2006b.
- Boehme, S. E., Sabine, C. L., and Reimers, C. E.: CO₂ fluxes from a coastal transect: a time-series approach, *Mar. Chem.*, 63, 49–67, 1998.
- Bowie, A. R., Whitworth, D. J., Achterberg, E. P., Fauzi, R., Mantoura, C., and Worsfold, P. J.: Biogeochemistry of Fe and other trace elements (Al, Co, Ni) in the upper Atlantic, *Deep-Sea Res.* I, 49, 605–636, 2002.
- Brea, S., Alvarez-Salgado, X. A., Alvarez, M., Pérez, F. F., Mémery, L., Mercier, H., and Messias, M. J.: Nutrient mineralization rates and ratios in the eastern South Atlantic, *J. Geophys. Res.*, 109, C05030, 1–15, doi:10.1029/2003JC002051, 2004.
- Bremner, J. M.: Concretionary phosphorite from SW Africa, *The Geological Society*, 137, 773–786, 1980.
- Bremner, J. M. and Willis, J. P.: Mineralogy and geochemistry of the clay fraction of sediments from the Namibian continental margin and the adjacent hinterland, *Mar. Geol.*, 115, 85–116, 1993.
- Broecker, W. S. and Peng, T. H.: Tracers in the sea, Palisades, N. Y.: Lamont-Doherty Geological Observatory, 1982.
- Bruland, K. W., Rue, L. E., Smith, G. J., and DiTullio, G. R.: Iron, macronutrients and diatom blooms in the Peru upwelling, *Mar. Chem.*, 93, 81–103, doi:10.1016/j.marchem.2004.06.011, 2005.
- Capone, D. G., Burns, J. A., Montoya, J. P., Subramaniam, A., Mahaffey, G., Gunderson, T., Michaels, A. F., and Carpenter, E. J.: Nitrogen fixation by *Trichodesmium* spp.: An important source of new nitrogen to the tropical and subtropical North Atlantic Ocean, *Global Biogeochem. Cy.*, 19, GB2024, doi:10.1029/2004GB002331, 2005.
- Carpenter, E. J.: Nitrogen fixation by marine Oscillatoria (*Trichodesmium*) in the world's oceans, in: Nitrogen in the Marine Environment, edited by: Carpenter, E. J. and Capone, D. G., Academic Press, New York, 65–103, 1983.
- Carr, M.-E.: Estimation of potential productivity in Eastern Boundary Currents using remote sensing, *Deep-Sea Res.* II, 49, 59–80, 2002.
- Deutsch, C., Sarmiento, J. L., Sigman, D. M., Gruber, N., and Dunne, J. P.: Spatial coupling of nitrogen inputs and losses in the ocean, *Nature*, 445, 163–167, doi:10.1038/nature05392, 2007.
- Dittmar, T. and Birkicht, M.: Regeneration of nutrients in the northern Benguela Upwelling and the Angola-Benguela Front Areas South African, *J. Sci.*, 97, 239–246, 2001.
- Duce, R. A., LaRoche, J., Altieri, K., Arrigo, K. R., Baker, A. R., Capone, D. G., Cornell, S., Dentener, F., Galloway, J., Ganeshram, R. S., Geider, R. J., Jickells, T., Kuypers, M. M., Langlois, R., Liss, P. S., Liu, S. M., Middelburg, J. J., Moore, C. M., Nickovic, S., Oschlies, A., Pedersen, T., Prospero, J., Schlitzer, R., Seitzinger, S., Sorensen, L. L., Uematsu, M., Ulloa, O., Voss, M., Ward, B., and Zamora, L.: Impacts of Atmospheric Anthropogenic Nitrogen on the Open Ocean, *Science*, 893, 893–897, doi:10.1126/science.1150369, 2008.
- Duncombe Rae, C. M.: A demonstration of the hydrographic partition of the Benguela upwelling ecosystem at 26°40' S, *Afr. J. Mar. Sci.*, 27, 617–628, 2005.
- Eckardt, F. D. and Kuring, N.: SeaWiFS identifies dust sources in the Namib Desert, *Int. J. Remote Sens.*, 26, 4159–4167, 2005.
- Emeis, K.-C., Brüchert, V., Currie, B., Endler, R., Ferdelman, T., Kiessling, A., Leipe, T., Noli-Pear, K., Struck, U., and Vogt, T.: Shallow gas in shelf sediments of the Namibian coastal upwelling ecosystem, *Cont. Shelf Res.*, 24, 627–642, 2004.
- Falkowski, P. G.: Evolution of the nitrogen cycle and its influence on the biological sequestration of CO₂ in the ocean, *Nature*, 387, 272–275, 1997.
- Föllmi, K. B.: The phosphorus cycle, phosphogenesis and marine phosphate-rich deposits, *Earth-Sci. Rev.*, 40, 55–124, 1996.
- Glenn, C. R., Föllmi, K. B., and Riggs, S. R.: Phosphorus and phosphorites: Sedimentology and environments of formation, *Eclogae Geol. Helv.*, 87, 747–788, 1994.
- Goldammer, T., Brüchert, V., Ferdelman, T. G., and Zabel, M.: Microbial sequestration of phosphorus in anoxic upwelling sediments, *Nat. Geosci.*, 3, 557–561, doi:10.1038/NGEO913, 2010.
- Goldammer, T., Brunner, B., Bernasconi, S. M., Ferdelman, T. G., and Zabel, M.: Phosphate oxygen isotopes: Insights into sedimentary phosphorus cycling from the Benguela upwelling system, *Geochim. Cosmochim. Ac.*, 75, 3741–3756, 2011.
- Gordon, A. L.: South Atlantic thermocline ventilation, *Deep-Sea Res.* I, 28, 1239–1264, 1981.
- Grasshoff, K., Kremling, K., and Ehrhardt, M.: Methods of seawater analysis, Third edition, edited by: Grasshoff, K., Kremling, K., and Ehrhardt, M., Verlag Chemie, 419 pp., 1999.
- Großkopf, T., Mohr, W., Baustian, T., Schunck, H., Gill, D., Kuypers, M. M. M., Lavik, G., Schmitz, R. A., R. Wallace, D. W., and LaRoche, J.: Doubling of marine dinitrogen-fixation rates based on direct measurements, *Nature*, 488, 361–364, doi:10.1038/nature11338, 2012.
- Gruber, N. and Sarmiento, J. L.: Global patterns of marine nitrogen fixation and denitrification, *Global Biogeochem. Cy.*, 11, 235–266, 1997.
- Hall, C. and Lutjeharms, J. R. E.: Cyclonic eddies identified in the Cape Basin of the South Atlantic Ocean, *J. Mar. Sys.*, 85, 1–10, doi:10.1016/j.jmarsys.2010.10.003, 2011.
- Heinze, C., Maier-Reimer, E., and Winn, K.: Glacial pCO₂ Reduction by the World Ocean: Experiments with the Hamburg Carbon Cycle Model, *Paleoceanography*, 6, 395–430, 1991.

- Hutchings, L., Lingen, C. D. v. d., Shannon, L. J., Crawford, R. J. M., Verheye, H. M. S., Bartholomae, C. H., Plas, A. K. v. d., Louw, D., Kreiner, A., Ostrowski, M., Fidel, Q., Barlow, R. G., Lamont, T., Coetzee, J., Shillington, F., Veitch, J., Currie, J. C., and Monteiro, P. M. S.: The Benguela Current: An ecosystem of four components, *Prog. Oceanogr.* 83, 15–32, 2009.
- Inthorn, M., Birch, G. F., Bremner, J. M., Calvert, S. E., and Rogers, J.: Compilation of organic carbon distribution and sedimentology in the surface sediments on the continental margin offshore southwestern Africa. Supplement to: Inthorn, M., Wagner, T., Scheeder, G., Zabel, M.: Lateral transport controls distribution, quality and burial of organic matter along continental slopes in high-productivity areas, *Geology*, 34, 205–208, doi:10.1130/G22153.1, 2006.
- Ito, T., Follows, M. J., and Boyle, E. A.: Is AOU a good measure of respiration in the oceans?, *Geophys. Res. Lett.*, 31, 1–4, doi:10.1029/2004GL020900, 2004.
- Jickells, T. D., An, Z. S., Andersen, K. K., Baker, A. R., Bergametti, G., Brooks, N., Cao, J. J., Boyd, P. W., Duce, R. A., Hunter, K. A., Kawahata, H., Kubilay, N., laRoche, J., Liss, P. S., Mahowald, N., Prospero, J. M., Ridgwell, A. J., Tegen, I., and Torres, R.: Global Iron Connections Between Desert Dust, Ocean Biogeochemistry and Climate Science, 308, 67–71, doi:10.1126/science.1105959, 2005.
- Johnson, K. S., Chavez, F. P., Elrod, V. A., Fitzwater, S. E., Pennington, J. T., Buck, K. R., and Walz, P. M.: The annual cycle of iron and the biological response in central California coastal waters, *Geophys. Res. Lett.*, 28, 1247–1250, 2001.
- Kalvelage, T., Jensen, M. M., Contreras, S., Revsbech, N. P., Lam, P., Günter, M., LaRoche, J., Lavik, G., and Kuypers, M. M. M.: Oxygen Sensitivity of Anammox and Coupled N-Cycle Processes in Oxygen Minimum Zones, *PLoS ONE*, 6, 1–12, doi:10.1371/journal.pone.0029299, 2011.
- Knapp, A. N.: The sensitivity of marine N_2 fixation to dissolved inorganic nitrogen, *Front. Microbiol.*, 3, 1–14, doi:10.3389/fmicb.2012.00374, 2012.
- Knapp, A. N., Dekaezemacker, J., Bonnet, S., Sohm, J. A., and Capone, D. G.: Sensitivity of *Trichodesmium erythraeum* and *Crocospaera watsonii* abundance and N_2 fixation rates to varying NO_3 and PO_4 concentrations in batch cultures, *Aquat. Microb. Ecol.*, 66, 223–236, doi:10.3354/ame01577, 2012.
- Koeve, W. and Kähler, P.: Heterotrophic denitrification vs. autotrophic anammox – quantifying collateral effects on the oceanic carbon cycle, *Biogeosciences*, 7, 2327–2337, doi:10.5194/bg-7-2327-2010, 2010.
- Krauk, J. M., Villareal, T. A., Sohm, J. A., Montoya, J. P., and Capone, D. G.: Plasticity of N:P ratios in laboratory and field populations of *Trichodesmium* spp., *Aquat. Microb. Ecol.*, 42, 243–253, 2006.
- Kuypers, M. M. M., Lavik, G., Woebken, D., Schmid, M., Fuchs, B. M., Amann, R., Jørgensen, B. B., and Jetten, M. S. M.: Massive nitrogen loss from the Benguela upwelling system through anaerobic ammonium oxidation, *PNAS* 102, 6478–6483, 2005.
- Lam, P. and Kuypers, M. M.: Microbial nitrogen cycling processes in oxygen minimum zones, *Annual Review in Marine Science*, 3, 317–345, doi:10.1146/annurev-marine-120709-142814, 2010.
- Li, Y.-H. and Peng, T.-H.: Latitudinal change of remineralization ratios in the oceans and its implication for nutrient cycles, *Global Biogeochem. Cy.*, 16, 1130, doi:10.1029/2001GB001828, 2002.
- Mahaffey, C., Williams, R. G., Wolff, G. A., Mahowald, N., Anderson, W., and Woodward, M.: Biogeochemical signatures of nitrogen fixation in the eastern North Atlantic, *Geophys. Res. Lett.*, 30, 3331–3334, doi:10.1029/2002GL016542, 2003.
- Mahaffey, C., Michaels, A. F., and Capone, D. G.: The conundrum of marine N_2 fixation, *Am. J. Sci.*, 305, 546–595, 2005.
- Mahowald, N. M., Engelstaedter, S., Luo, C., Sealy, A., Artaxo, P., Benitez-Nelson, C., Bonnet, S., Chen, Y., Chuang, P. Y., Cohen, D. D., Dulac, F., Herut, B., Johansen, A. M., Kubilay, N., Losno, R., Maenhaut, W., Paytan, A., Prospero, J. M., Shank, L. M., and Siefert, R. L.: Atmospheric Iron Deposition: Global Distribution, Variability, and Human Perturbations, *Annu. Rev. Mar. Sci.*, 1, 245–278, doi:10.1146/annurev.marine.010908.163727, 2009.
- McElroy, M. B.: Marine biological controls on atmospheric CO_2 and climate, *Nature*, 302, 328–329, 1983.
- Meeuwis, J. M. and Lutjeharms, J. R. E.: Surface thermal characteristics of the Angola-Benguela Front, *S. Afr. J. Marine Sci.*, 9, 261–279, 1990.
- Mills, M. M., Ridame, C., Davey, M., La Roche, J., and Geider, R. J.: Iron and phosphorus co-limit nitrogen fixation in the eastern tropical North Atlantic, *Nature*, 429, 292–294, doi:10.1038/nature02550, 2004.
- Mintrop, L.: The Versatile Instrument for the Determination of Titration Alkalinity: Manual for version 3s and 3c, Marianda 2, 2005.
- Mohr, W., Großkopf, T., Wallace, D. W. R., and La Roche, J.: Methodological underestimation of oceanic nitrogen fixation rates, *PLoS ONE*, 5, e12583, doi:10.1371/journal.pone.0012583, 2010.
- Mohrholz, V., Bartholomae, C. H., Plas, A. K. v. d., and Lass, H. U.: The seasonal variability of the northern Benguela undercurrent and its relation to the oxygen budget on the shelf, *Cont. Shelf Res.*, 28, 424–441, 2008.
- Moisander, P. H., Beinart, R. A., Hewson, I., White, A. E., Johnson, K. S., Carlson, C. A., Montoya, J. P., and Zehr, J. P.: Unicellular Cyanobacterial Distributions Broaden the Oceanic N_2 Fixation Domain, *Science*, 327, 1512–1514, doi:10.1126/science.1185468, 2010.
- Monteiro, P. M. S., Plas, A. v. d., Mohrholz, V., Mabilile, E., Pascall, A., and Joubert, W.: Variability of natural hypoxia and methane in a coastal upwelling system: Oceanic physics or shelf biology?, *Geophys. Res. Lett.*, 33, L16614, doi:10.1029/2006GL026234, 2006.
- Moore, C. M., Mills, M. M., Achterberg, E. P., Geider, R. J., LaRoche, J., Lucas, M. I., McDonagh, E. L., Pan, X., Poulton, A. J., Rijkenberg, M. J. A., Suggett, D. J., Ussher, S. J., and Woodward, E. M.: Large-scale distribution of Atlantic nitrogen fixation controlled by iron availability, *Nat. Geosci.*, 2, 867–871, doi:10.1038/NGEO667, 2009.
- Nagel, B., Emeis, K.-C., Flohr, A., Rixen, T., Schlarbaum, T., Mohrholz, V., and v. d. Plas, A.: N-cycling and balancing of the N-deficit generated in the oxygen minimum zone over the Namibian shelf – an isotope-based approach, *Journal of Geophysical Research: Biogeosciences*, 118, 361–371, doi:10.1002/jgrg.20040, 2013.
- Nathan, Y., Bremner, J. M., E., R., Loewenthal, and Monteiro, P.: Role of bacteria in phosphorite genesis, *Geomicrobiol. J.*, 11, 69–76, doi:10.1080/01490459309377935, 1993.

- Noble, A. E., Lamborg, C. H., Ohnemus, D. C., Lam, P. J., Goepfert, T. J., Measures, C. I., Frame, C. H., Casciotti, K. L., DiTullio, G. R., Jennings, J., and Saito, M. A.: Basin-scale inputs of cobalt, iron, and manganese from the Benguela-Angola front to the South Atlantic Ocean, *Limnol. Oceanogr.*, 57, 989–1010, doi:10.4319/lo.2012.57.4.0989, 2012.
- Poole, R. and Tomczak, M.: Optimum multiparameter analysis of the water mass structure in the Atlantic Ocean thermocline, *Deep-Sea Res. I*, 46, 1895–1921, 1999.
- Redfield, A. C., Ketchum, B. H., and Richards, F. A.: The influence of organisms on the composition of seawater, *The Sea*, edited by: Hill, M. N. E., Wiley – Interscience New York, 1963.
- Riebesell, U., Schulz, K. G., Bellerby, R. G. J., Botros, M., Fritsche, P., Meyerhöfer, M., Neill, C., Nondal, G., Oschlies, A., Wohlers, J., and Zöllner, E.: Enhanced biological carbon consumption in a high CO₂ ocean, *Nature*, 450, 545–549, doi:10.1038/nature06267, 2007.
- Saito, M. A., Moffet, J. M., Chisholm, S. W., and Waterbury, J. B.: Cobalt limitation and uptake in *Prochlorococcus*, *Limnol. Oceanogr.*, 47, 1629–1636, 2002.
- Saito, M. A., Moffet, J. M., and DiTullio, G. R.: Cobalt and Nickel in the Peru upwelling region: A major flux of labile cobalt utilized as a micronutrient, *Global Biogeochem. Cy.*, 18, GB4030, doi:10.1029/2003GB002216, 2004.
- Sarthou, G., Baker, A. R., Blain, S., Achterberg, E. P., Boye, M., Bowie, A. R., Croot, P., Laan, P., Baar, H. J. W. d., Jickells, T. D., and Worsfold, P. J.: Atmospheric iron deposition and sea-surface dissolved iron concentrations in the eastern Atlantic Ocean, *Deep-Sea Res. I*, 50, doi:10.1016/S0967-0637(03)00126-2, 2003.
- Schneider, B., Schlitzer, R., Fischer, G., and Nöthig, E.-M.: Depth-dependent elemental compositions of particulate organic matter (POM) in the ocean, *Global Biogeochem. Cy.*, 17, 1–16, doi:10.1029/2002GB001871, 2003.
- Schulz, H. N. and Schulz, H. D.: Large Sulfur Bacteria and the Formation of Phosphorite, *Science*, 307, 416–418, 2005.
- Shannon, L. V.: The Benguela Ecosystem: 1. evolution of the Benguela, physical features and processes, *Oceanogr. Mar. Biol.*, 23, 105–182, 1985.
- Shillington, F., Reason, C. J. C., Duncombe Rae, C. M., Florenchie, P., and Penven, P.: Large scale physical variability of the Benguela Current Large Marine Ecosystem (BCLME), in: *Benguela: predicting a large marine ecosystem*, edited by: Shannon, V., Hempel, G., Malanotte-Rizzoli, P., Moloney, C., and Woods, J., Large marine ecosystems Elsevier, Amsterdam, 2006.
- Singh, A., Lomas, M. W., and Bates, N. R.: Revisiting N₂ fixation in the North Atlantic Ocean: Significance of deviations from the Redfield Ratio, atmospheric deposition and climate variability, *Deep-Sea Res. II*, 93, 148–158, doi:10.1016/j.dsr2.2013.04.008, 2013.
- Sohm, J. A., Hilton, J. A., Noble, A. E., Zehr, J. P., Saito, M. A., and Webb, E. A.: Nitrogen fixation in the South Atlantic Gyre and the Benguela Upwelling System, *Geophys. Res. Lett.*, 38, 1–6, doi:10.1029/2011GL048315, 2011.
- Staal, M., te Lintel Hekkert, S., Brummer, G. J., Veldhuis, M., Sikkens, C., Persijn, S., and Stal, L. J.: Nitrogen fixation along a north-south transect in the eastern Atlantic Ocean, *Limnol. Oceanogr.*, 52, 1305–1316, 2007.
- Stramma, L. and England, S.: On the water masses and mean circulation of the South Atlantic Ocean, *J. Geophys. Res.*, 104, 20863–20883, 1999.
- Subramaniam, A., Mahaffey, C., Johns, W., and Mahowald, N.: Equatorial upwelling enhances nitrogen fixation in the Atlantic Ocean, *Geophys. Res. Lett.*, 40, 1766–1771, doi:10.1002/grl.50250, 2013.
- Swap, R., Garstang, M., Macko, S. A., Tyson, P. D., Maenhaut, W., Artaxo, P., Kallberg, P., and Talbot, R.: The long-range transport of southern African aerosols to the tropical South Atlantic, *J. Geophys. Res.*, 101, 23777–23791, 1996.
- Takahashi, T., Broecker, W., and Langer, S.: Redfield Ratio Based on Chemical Data from Isopycnal Surfaces, *J. Geophys. Res.*, 90, 6907–6924, 1985.
- Torres, R., Turner, D. R., Silva, N., and Rutllant, J.: High short-term variability of CO₂ fluxes during an upwelling event off the Chilean coast at 30° S, *Deep-Sea Res. I*, 46, 1161–1179, 1999.
- Tyrrell, T. and Law, C. S.: Low nitrate:phosphate ratios in the global ocean, *Nature*, 387, 793–796, 1997.
- Tyrrell, T. and Lucas, M. I.: Geochemical evidence of denitrification in the Benguela upwelling system, *Cont. Shelf Res.*, 22, 2497–2511, 2002.
- Tyrrell, T., Maranon, E., Poulton, A. J., Bowie, A. R., and Harbour, D. S.: Large-scale latitudinal distribution of *Trichodesmium* spp. in the Atlantic Ocean, *J. Plankton Res.*, 25, 405–416, 2003.
- Tyson, P. D., Garstang, M., Swap, R., Kallberg, P., and Edwards, M.: An air transport climatology for subtropical southern Africa, *Int. J. Climatol.*, 16, 265–291, 1996.
- van der Plas, A. K., Monteiro, P. M. S., and Pascall, A.: Cross-shelf biogeochemical characteristics of sediments in the central Benguela and their relationship to overlying water column hypoxia, *Afr. J. Marine Sci.*, 29, 37–47, 2007.
- Watson, A. J., Bakker, D. C. E., Ridgwell, A. J., Boyd, P. W., and Law, C. S.: Effect of iron supply on Southern Ocean CO₂ uptake and implications for glacial atmospheric CO₂, *Nature*, 407, 730–733, 2000.
- Weeks, S. J., Currie, B., and Bakun, A.: Massive emissions of toxic gas in the Atlantic, *Nature*, 415, 493–494, 2002.
- Weiss, R. F.: The solubility of nitrogen, oxygen and argon in water and seawater, *Deep Sea Res.*, 17, 721–735, 1970.
- Zehr, J. P.: Nitrogen fixation by marine cyanobacteria, *Trends in Microbiology*, 19, 162–173, doi:10.1016/j.tim.2010.12.004, 2011.